

## Electronic Supplementary Information

# Unusual Chemistry of Cu(II) Salan Complexes: Synthesis, Characterization and Superoxide Dismutase Activity

Satabdi Roy,<sup>a</sup> Atanu Banerjee,<sup>a</sup> Sudhir Lima,<sup>a</sup> Adolfo Horn Jr.,<sup>b,c</sup> Raquel M. S. N. Sampaio,<sup>b</sup> Nádia Ribeiro,<sup>d</sup> Isabel Correia,<sup>d</sup> Fernando Avecilla,<sup>e</sup> M. Fernanda N. N. Carvalho,<sup>d</sup> Maxim L. Kuznetsov,<sup>d</sup> João Costa Pessoa<sup>\*d</sup> Werner Kaminsky<sup>f</sup> and Rupam Dinda<sup>\*a</sup>

<sup>a</sup> Department of Chemistry, National Institute of Technology, Rourkela 769008, Odisha, India.

<sup>b</sup> Laboratório de Ciências Químicas, Universidade Estadual do Norte Fluminense Darcy Ribeiro, 28013-602, Campos do Goytacazes, RJ, Brazil.

<sup>c</sup> Universidade Federal de Santa Catarina, Campus Universitário Trindade, 88040-900 Florianópolis, SC, Brazil.

<sup>d</sup> Centro de Química Estrutural and Departamento de Engenharia Química, Instituto Superior Técnico, Universidade de Lisboa, Avenida Rovisco Pais, 1049-001, Lisboa, Portugal

<sup>e</sup> Grupo Xenomar, Centro de Investigacións Científicas Avanzadas (CICA), Departamento de Química, Facultade de Ciencias, Universidade da Coruña, Campus de A Coruña, 15071A Coruña, Spain.

<sup>f</sup> Department of Chemistry, University of Washington, Seattle, Washington 98195, United States

## Electronic spectral data for complexes

Table S1 Electronic spectral data for complexes 1-4 in DMSO.

Complexes	$\lambda_{\text{max}}/\text{nm}$ ( $\epsilon/\text{M}^{-1} \text{cm}^{-1}$ )
1	296 (15109), 352 (2121), 424 (2445), 609 (657)
2	286 (23121), 344 (2023), 424 (2788), 613 (589)
3	295 (20338), 397 (1555), 429 (2223), 605 (770)
4	294 (11384), 371 (1563), 419 (2312), 601 (431)

## Supplementary single crystal X-ray diffraction data.

Table S2(a) Selected bond parameters in  $\text{H}_2\text{L}^3$ .

Bond lengths ( $\text{\AA}$ )			
O(1)-C(10)	1.367(2)	N(1)-C(4)	1.485(3)
O(2)-C(21)	1.367(2)	N(1)-C(3)	1.461(2)
N(2)-C(25)	1.468(3)	N(2)-C(3)	1.465(2)
Bond angles ( $^\circ$ )			
N(1)-C(3)-N(2)	104.44(15)	N(2)-Cu(1)-O(2)	92.2(2)

Table S2(b) Intramolecular hydrogen bonds in compound  $\text{H}_2\text{L}^3$ .

D-H...A	d(D-H)	d(H...A)	d(D...A)	$\angle(\text{DHA})$
O(1)-H(10)...N(1)	0.84(3)	1.83(3)	2.615(2)	155(3)
O(2)-H(20)...N(2)	0.90(3)	1.80(3)	2.628(2)	153(3)

Table S3 Selected geometric parameters (Å, °) for the Cu-complexes **1A**, **3** and **4**

[Cu(L <sup>1</sup> )(DMSO)] ( <b>1A</b> )			
Bond lengths (Å)			
N(1)-Cu(1)	2.054(7)	N(2)-Cu(1)	2.047(5)
O(1)-Cu(1)	1.863(5)	O(2)-Cu(1)	1.901(5)
O(3)-Cu(1)	2.41(1)		
Bond angles (°)			
N(1)-Cu(1)-N(2)	86.0(3)	N(2)-Cu(1)-O(2)	92.2(2)
N(1)-Cu(1)-O(1)	91.3(2)	N(2)-Cu(1)-O(3)	89.7(3)
N(1)-Cu(1)-O(2)	162.8(2)	O(1)-Cu(1)-O(2)	88.2(2)
N(1)-Cu(1)-O(3)	97.3(3)	O(1)-Cu(1)-O(3)	98.1(3)
N(2)-Cu(1)-O(1)	172.0(2)	O(2)-Cu(1)-O(3)	99.8(3)
N(1)-Cu(1)-N(2)	86.0(3)	N(2)-Cu(1)-O(2)	92.2(2)
[Cu(L <sup>3A</sup> )] <sub>2</sub> ( <b>3</b> )			
Bond lengths (Å)			
O(1)-Cu(1)	1.971(8)	N(1)-Cu(1)	1.968(10)
O(2)-Cu(1)	1.909(8)	N(2)-Cu(1)	2.042(9)
O(1 <sup>i</sup> )-Cu(1)	2.786(10)	O(3)-Cu(1)	2.544(9)
Cu(1)-Cu(1 <sup>i</sup> )	3.732(4)	Cu(2)-Cu(2 <sup>i</sup> )	3.381(3)
Bond angles (°)			
O(2)-Cu(1)-N(1)	151.5(4)	O(2)-Cu(1)-O(1)	100.2(3)
N(1)-Cu(1)-O(1)	91.3(4)	O(2)-Cu(1)-N(2)	91.9(4)
N(1)-Cu(1)-N(2)	86.2(4)	O(1)-Cu(1)-N(2)	158.7(4)
[Cu(L <sup>4A</sup> )] ( <b>4</b> )			
Bond lengths (Å)			
N(2)-Cu(1)	2.002(2)	O(2)-Cu(1)	1.896(3)
N(1)-Cu(1)	2.052(3)	O(1)-Cu(1)	1.878(2)
Bond angles (°)			
N(2)-Cu(1)-N(1)	85.8(1)	N(1)-Cu(1)-O(2)	173.4(1)
N(2)-Cu(1)-O(2)	92.9(1)	N(1)-Cu(1)-O(1)	93.2(1)
N(2)-Cu(1)-O(1)	170.2(1)	O(2)-Cu(1)-O(1)	89.1(1)

**$^1\text{H}$  and  $^{13}\text{C}$  NMR spectra of ligand precursor**

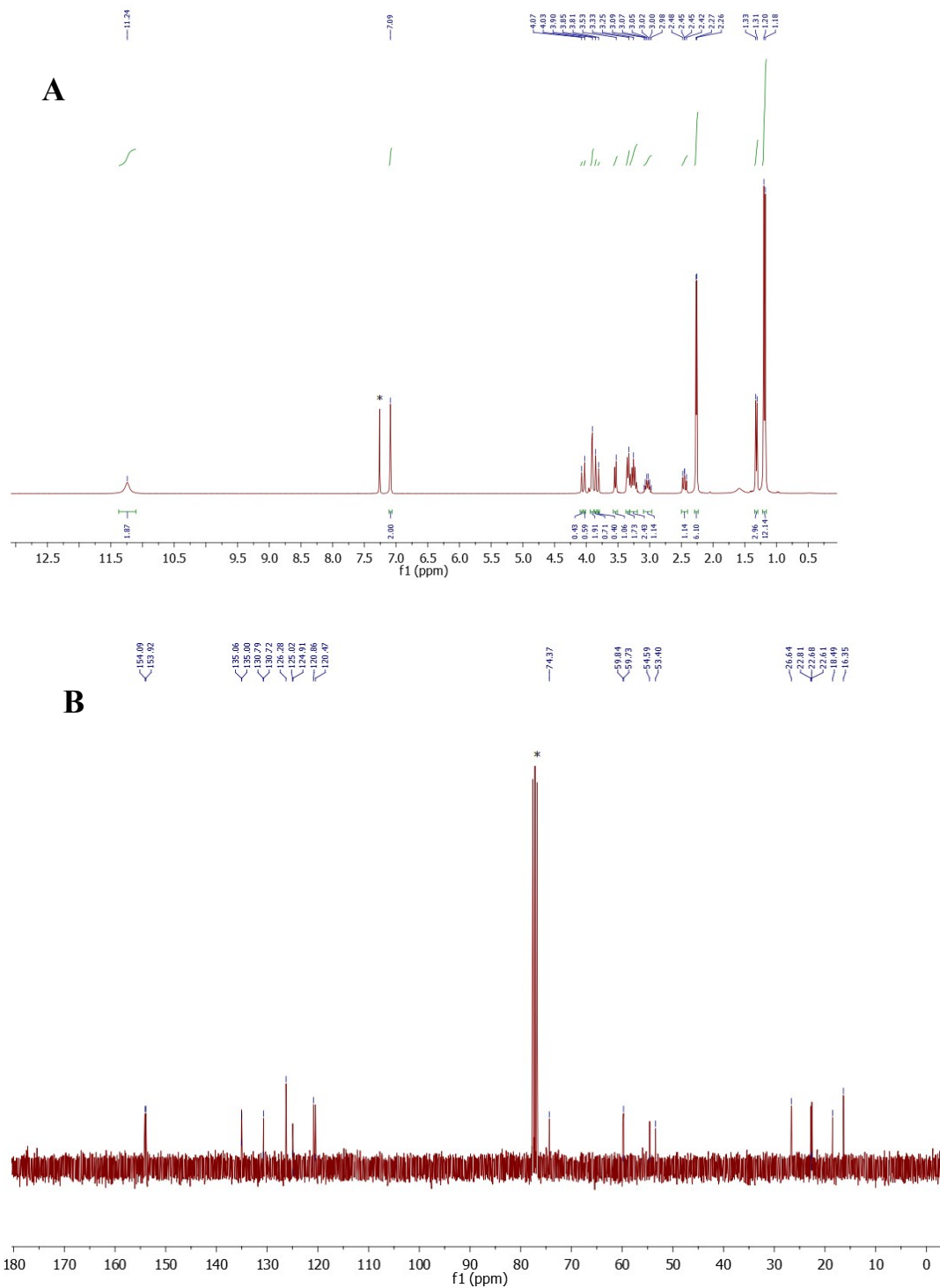


Fig. S1  $^1\text{H}$  NMR (A) and  $^{13}\text{C}$  NMR (B) spectrum of  $\text{H}_2\text{L}^3$  in  $\text{CDCl}_3$  (\* marks the solvent signal).

## ESI-MS spectra

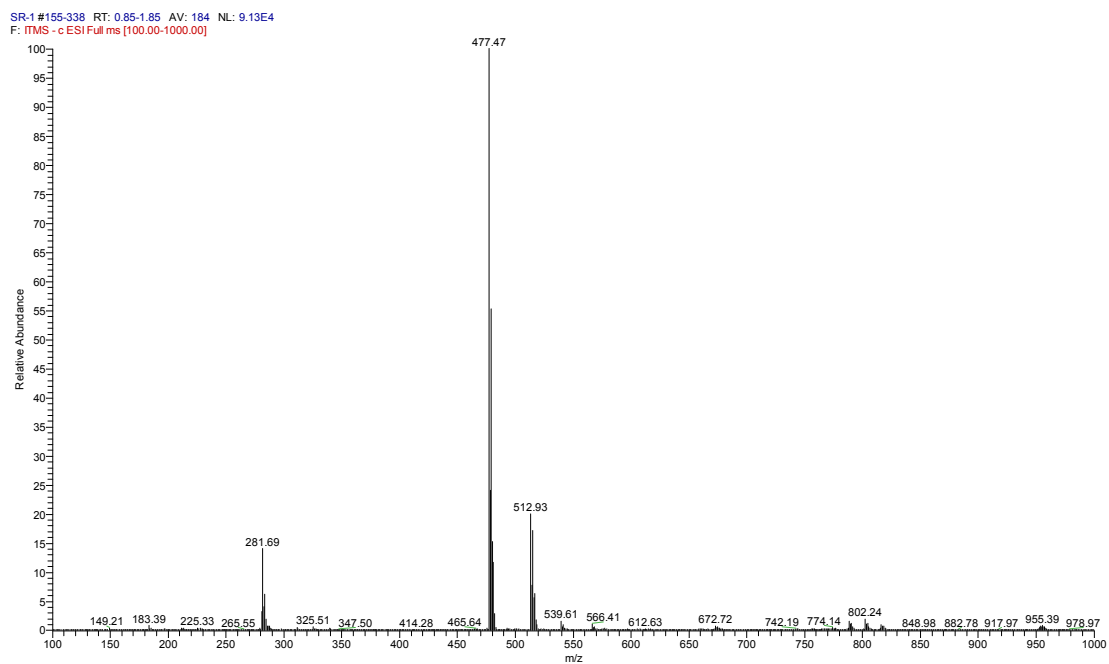


Fig. S2(a) ESI-MS spectrum of  $H_2L^3$  in the negative ion mode (MeOH solution).

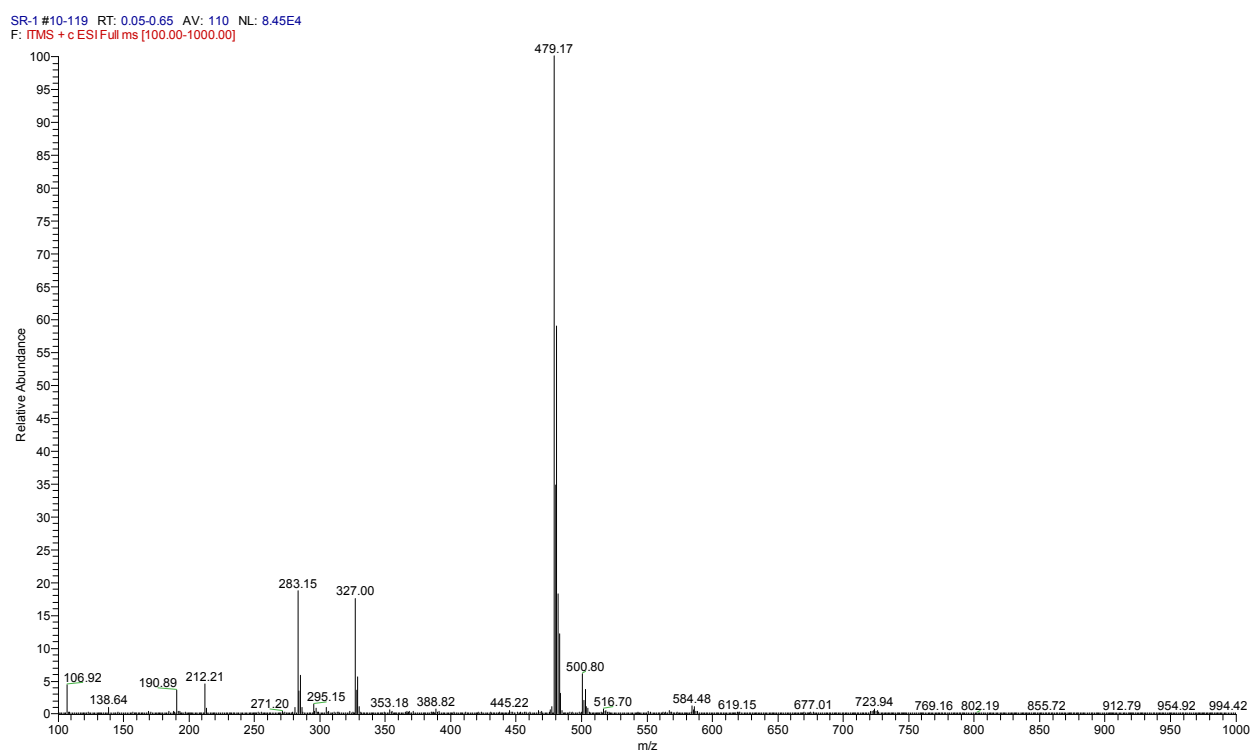


Fig. S2(b) ESI-MS spectrum of  $H_2L^3$  in the positive ion mode (MeOH solution).

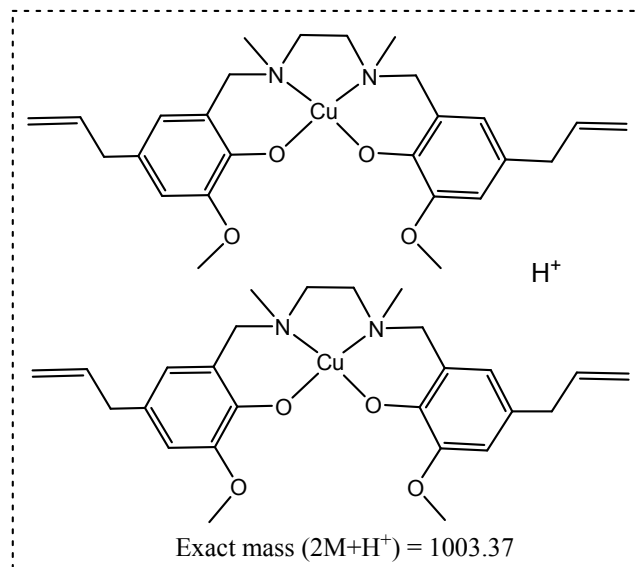


Fig. S3 Proposed molecular formulae for species found in the ESI-MS spectrum of **2**.

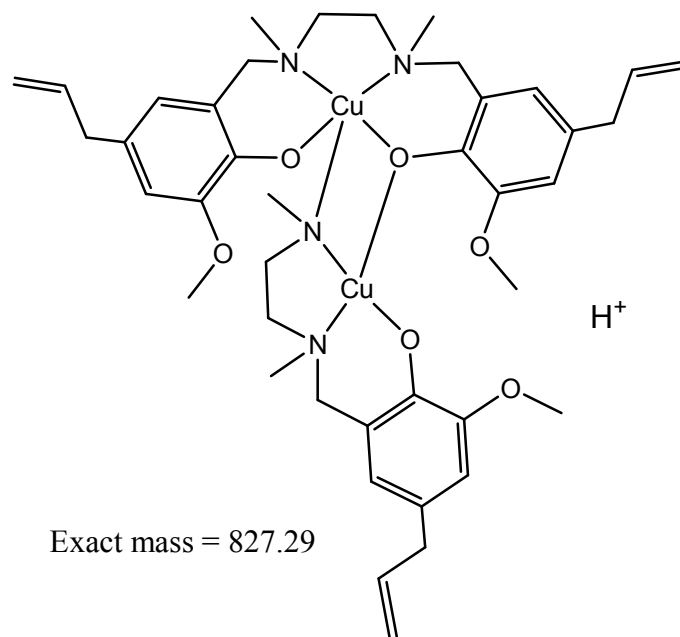


Fig. S4 Proposed molecular formulae for deaminated species found in the ESI-MS spectrum of **2**.

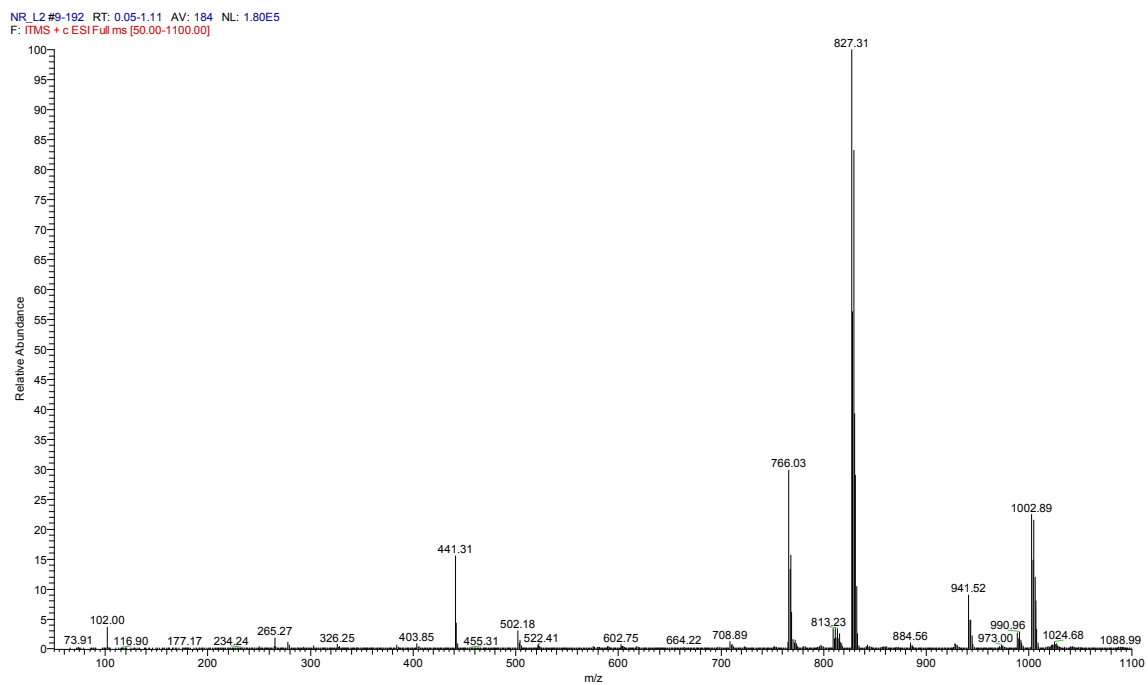


Fig. S5 ESI-MS spectrum of **2** in the positive ion mode (MeOH solution).

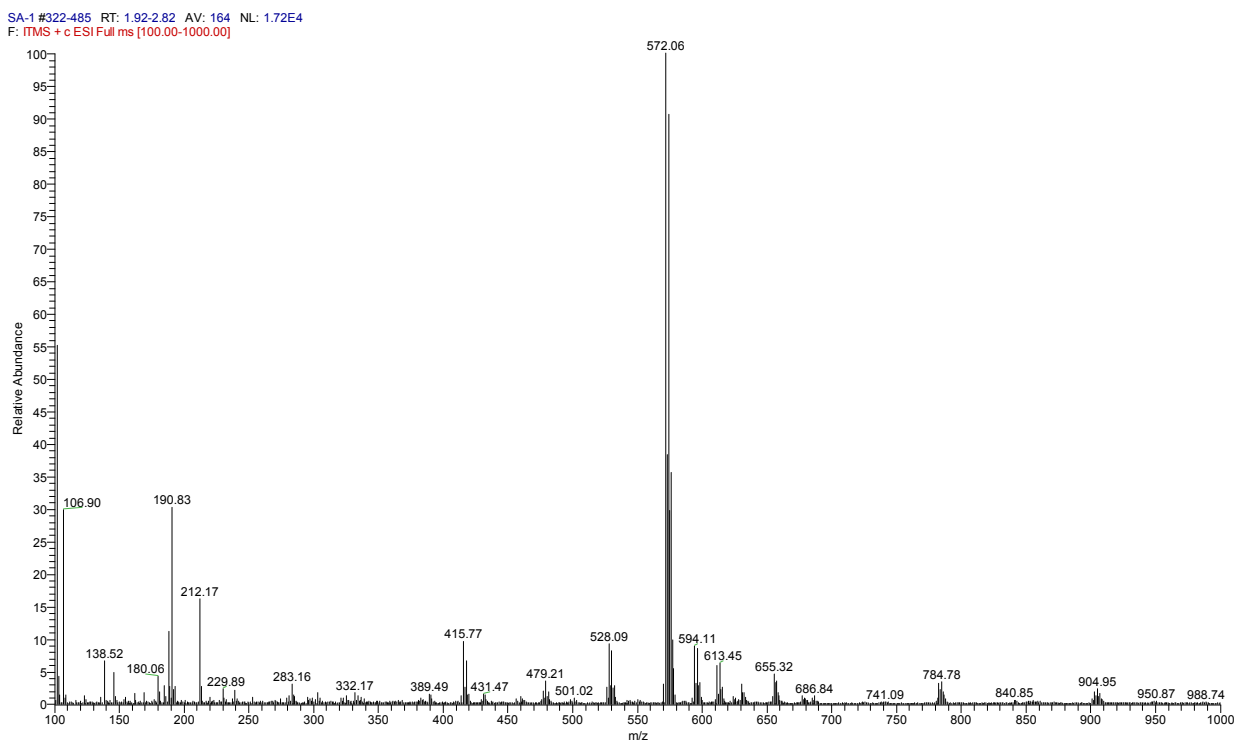


Fig. S6 ESI-MS spectrum of **3** in the positive ion mode (MeOH solution).

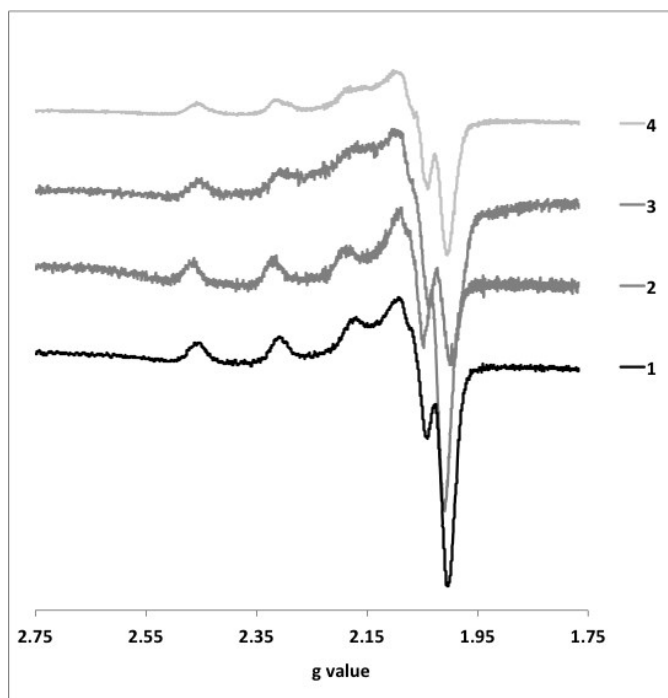


Fig. S7 First derivative EPR spectra of frozen solutions of the Cu-complexes **1-4** in DMF (*ca.* 3 mM), measured at *ca.* 100 K.

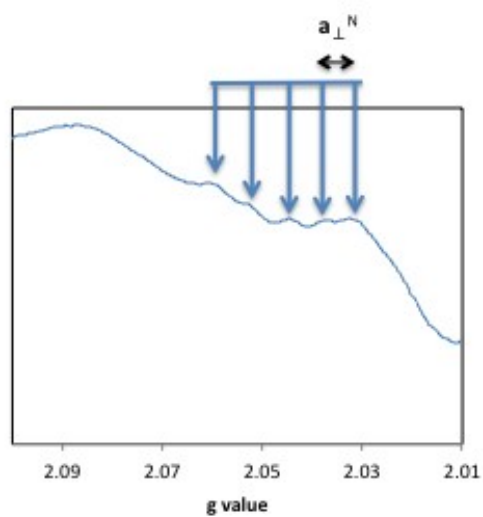
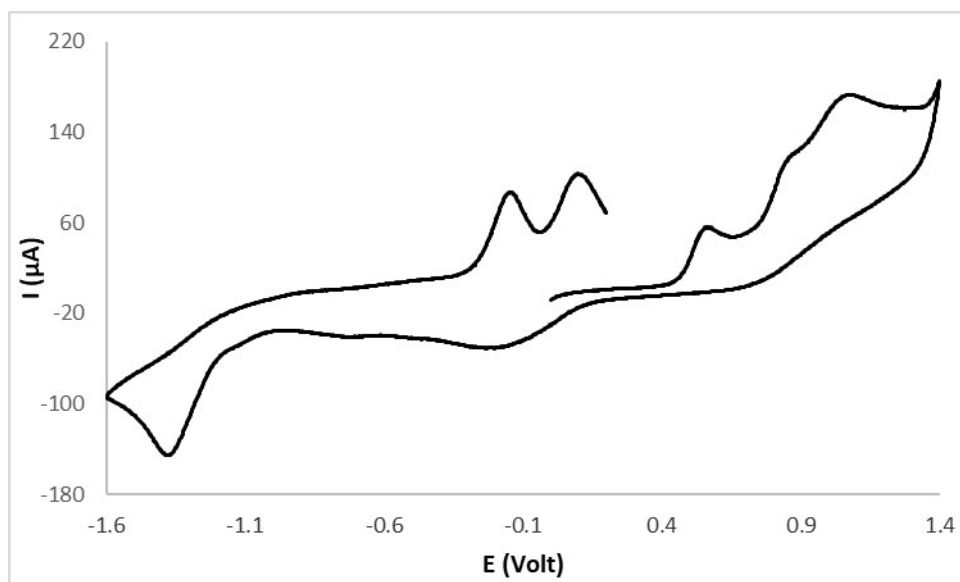


Fig S8 X-band EPR spectrum of **4** evidencing the superhyperfine structure in the perpendicular region resulting from spin-coupling of the unpaired electron with two  $^{14}\text{N}$  nuclei.



## Additional Electrochemical data

a)



b)

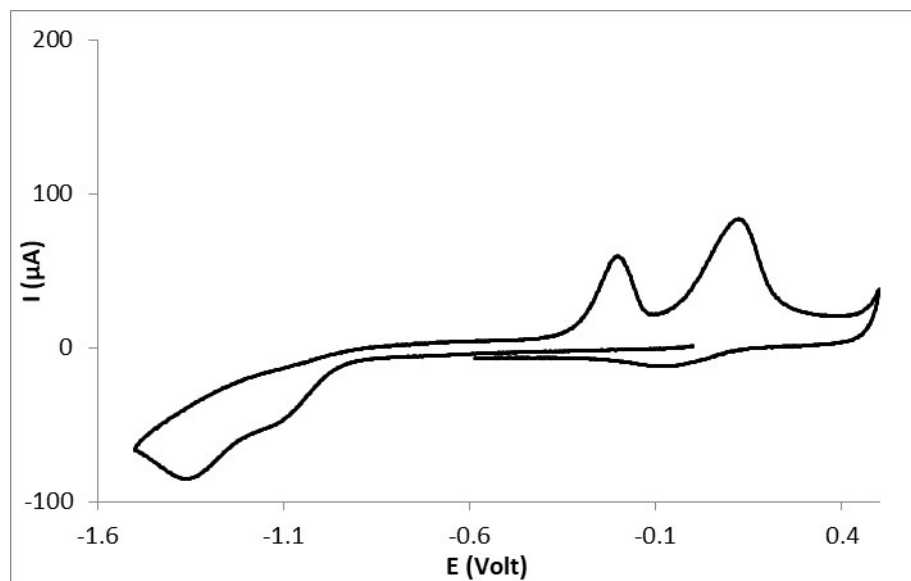
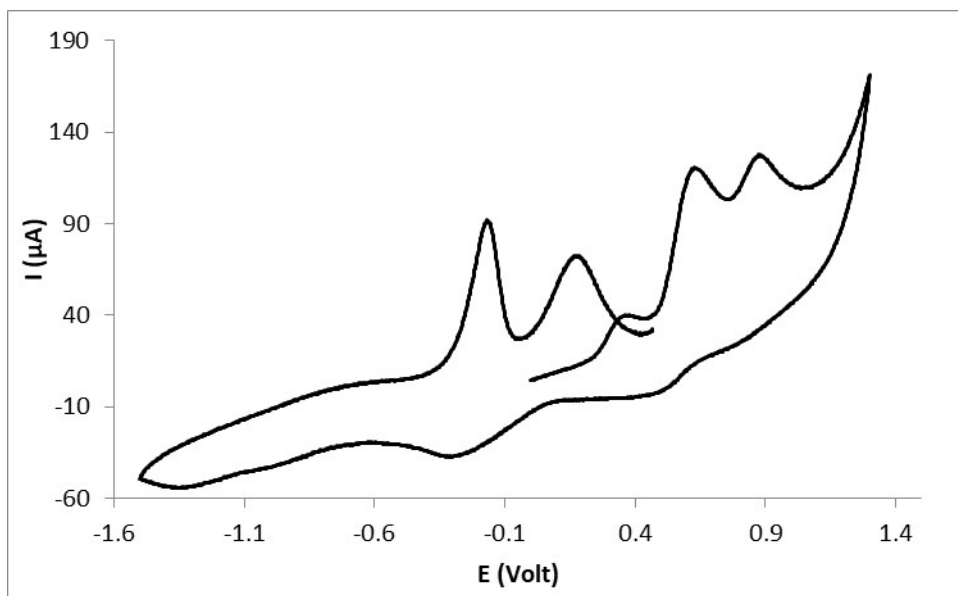


Fig. S9 Cyclic voltammogram of complex **1**. (a) anodic scan; (b) cathodic scan. The cyclic voltammograms were obtained in  $\text{NBu}_4\text{BF}_4/\text{DMF}$  (0.1 M) at 200 mV/s.

a)



b)

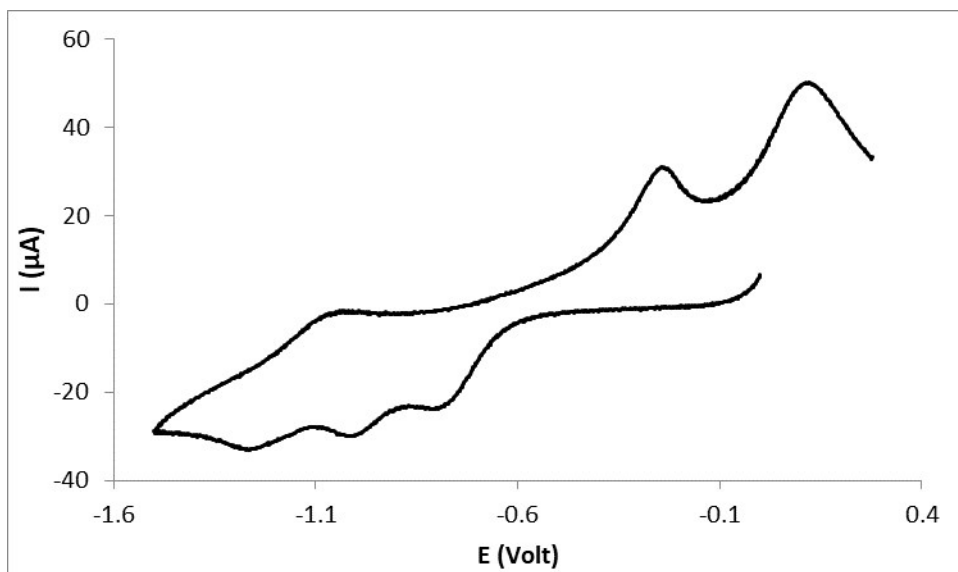
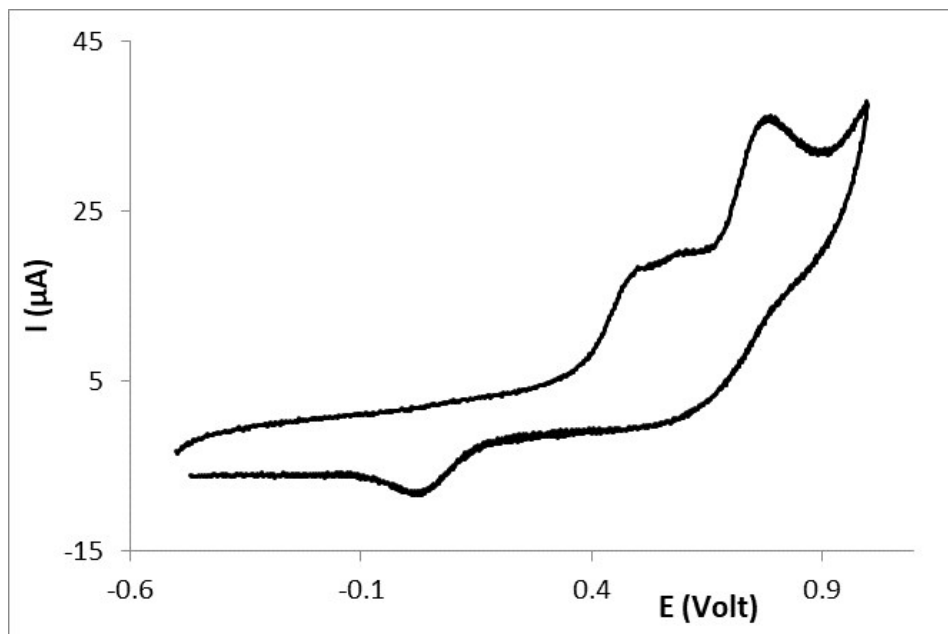


Fig. S10 Cyclic voltammogram of complex **2**. (a) anodic scan; (b) cathodic scan. The cyclic voltammograms were obtained in  $\text{NBu}_4\text{BF}_4/\text{DMF}$  (0.1M) at 200 mV/s.

a)



b)

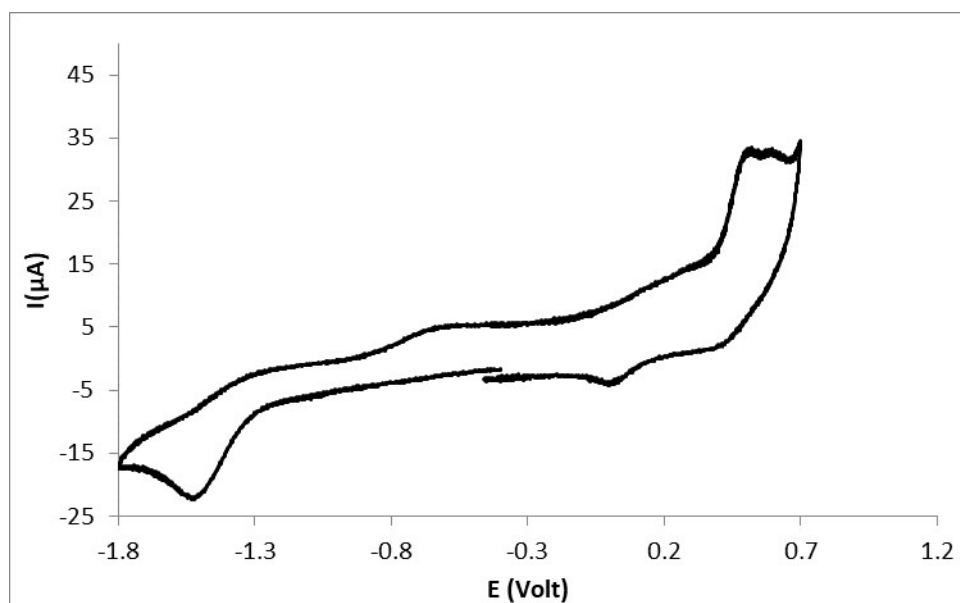
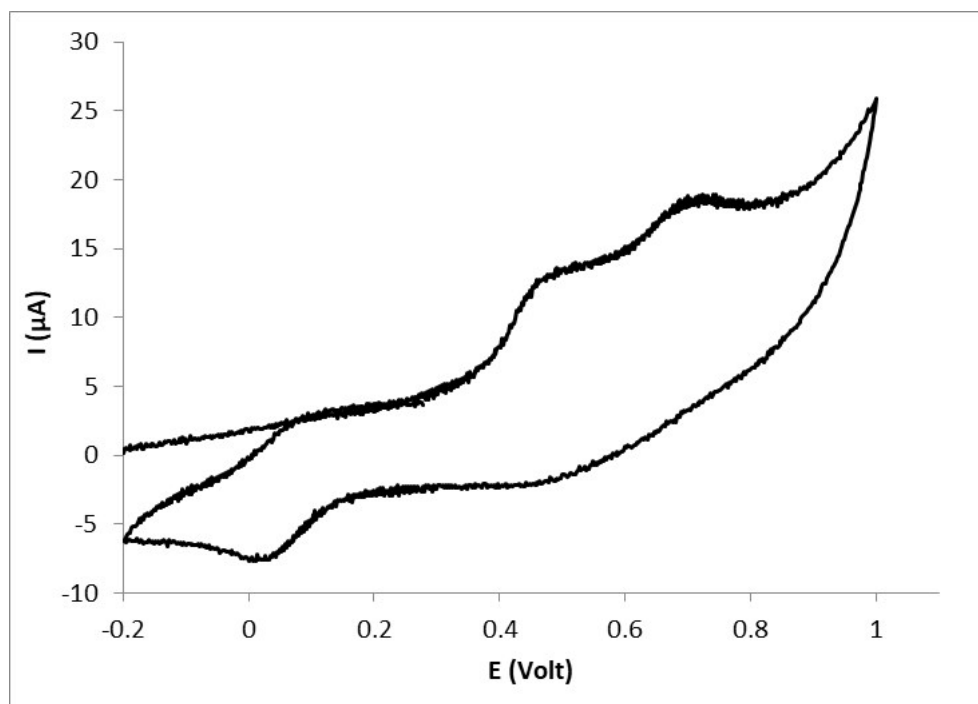


Fig. S11 Cyclic voltammogram of complex 3. (a) anodic scan; (b) cathodic scan. The cyclic voltammograms were obtained in  $\text{NBu}_4\text{BF}_4/\text{DMF}$  (0.1M) at 200 mV/s.

a)



b)

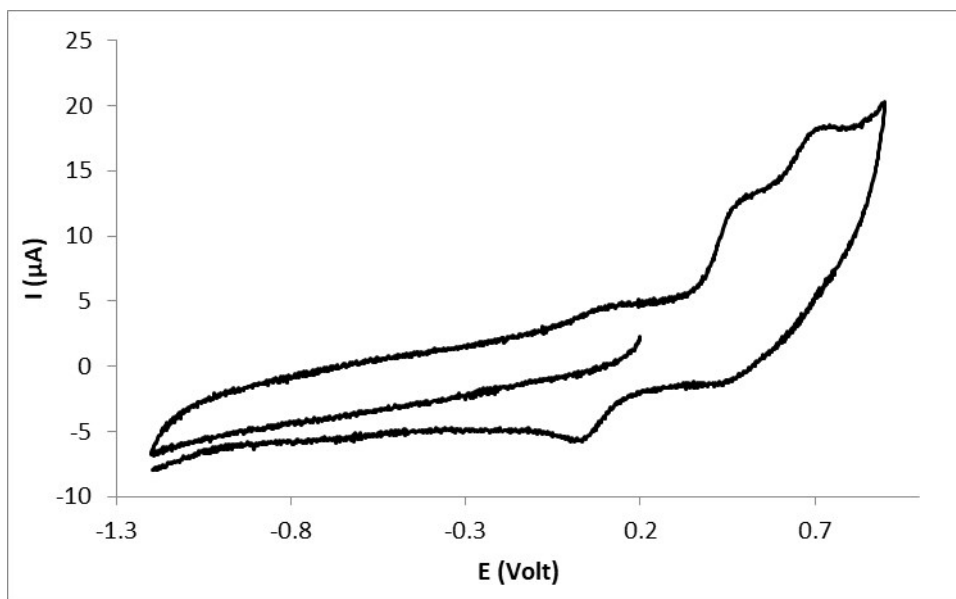


Fig. S12 Cyclic voltammogram of complex 4. (a) anodic scan; (b) cathodic scan. The cyclic voltammograms were obtained in  $\text{NBu}_4\text{BF}_4/\text{DMF}$  (0.1M) at 200 mV/s.

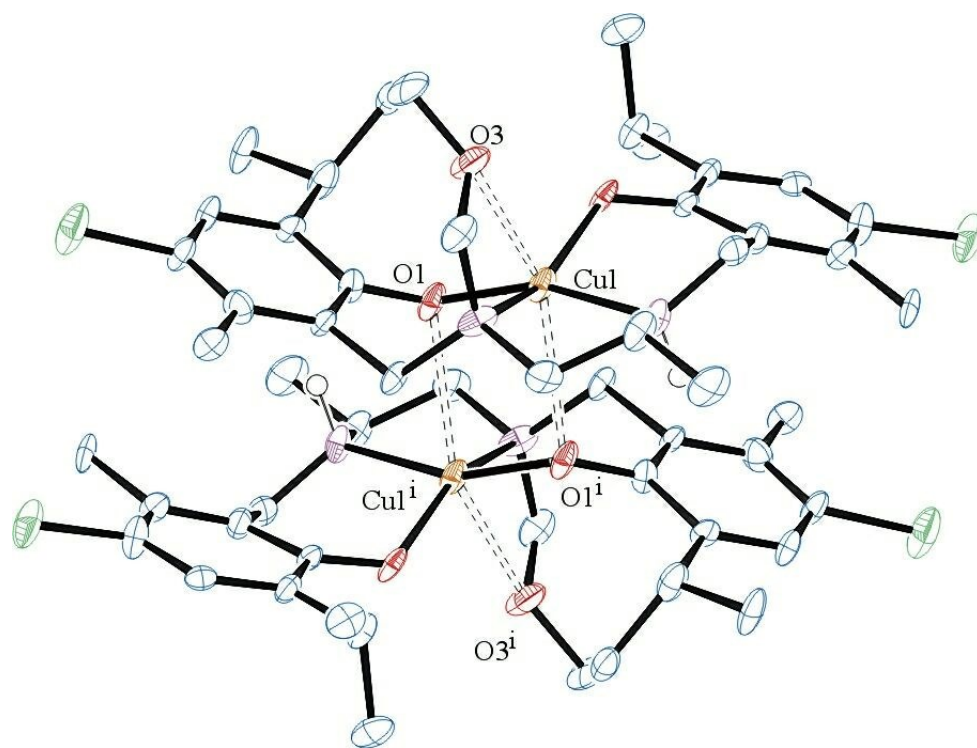


Fig. S13 ORTEP diagram of  $[\text{Cu}(\text{L}^{3\text{A}})]_2$  (**3**) showing the weak interactions 50% probability level (Bond distance,  $\text{Cu(1)-Cu(1}^i\text{)} = 3.732(4) \text{ \AA}$ )

## Evaluation of Superoxide dismutase activity

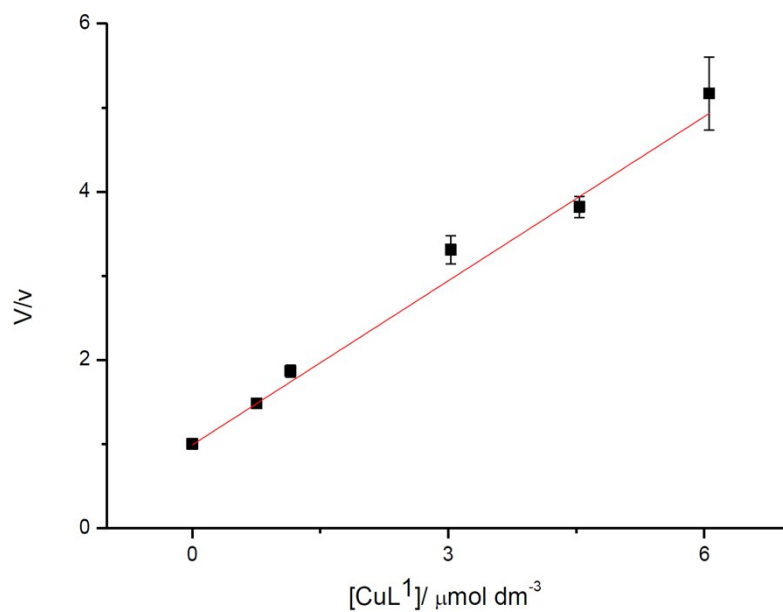


Fig. S14 Plot of  $V/v$  vs. complex concentration of  $[\text{CuL}^1]$  (**1**) employed for  $\text{IC}_{50}$  calculation.  $V/v$  is the ratio between the NBT reduction rate in the absence ( $V$ ) and in the presence ( $v$ ) of different concentration of complex **1**. The  $\text{IC}_{50}$  is the value at  $V/v = 2$ .

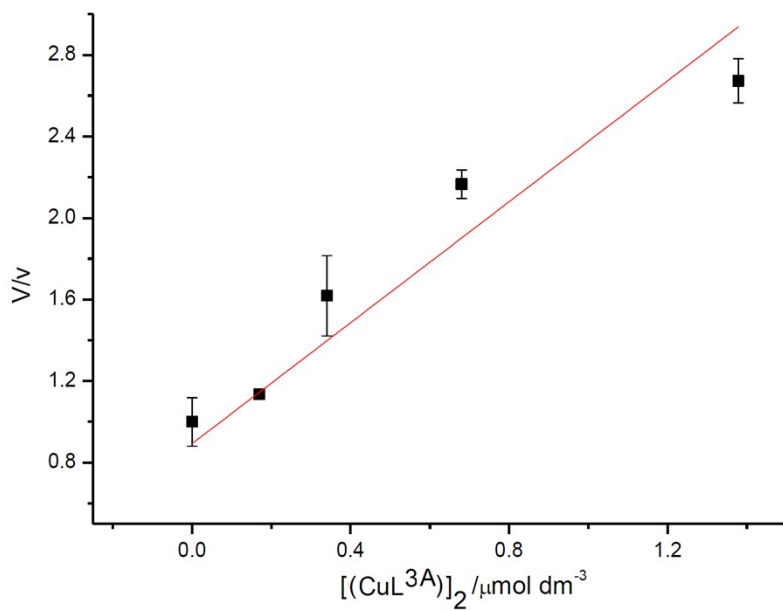


Fig. S15 Plot of  $V/v$  vs. complex concentration of  $[(\text{CuL}^{3\text{A}})]_2$  (**3**) employed for  $\text{IC}_{50}$  calculation.  $V/v$  is the ratio between the NBT reduction rate in the absence ( $V$ ) and in the presence ( $v$ ) of different concentration of complex **3**. The  $\text{IC}_{50}$  is the value at  $V/v = 2$ .